Design, Synthesis, Physicochemical and Antimicrobial Properties of Rhenium(I) tricarbonyl complexes of 3-(phenylimino)indole-2-one

A. A. Ikotun[1*], M. P. Coogan[2], A. A. Owoseni[3] and G. O. Egharevba[4]
[1]Department of Chemistry and Industrial Chemistry, Bowen University, Iwo, Nigeria.;
[2]Department of Chemistry, Cardiff University, Wales, United Kingdom; [3]Department of Biological Sciences, Bowen University, Iwo, Nigeria;
[4]Department of Chemistry, Obafemi Awolowo University, Ile-Ife, Nigeria

[*] Corresponding Author: ikotunadebomi@gmail.com, +2348035856562
Received 14 July 2019; accepted 17 August 2019, published online 29 August 2019

Abstract
Modern medical application of luminescent d^6 transition metal complexes to cell imaging has aroused great interest. Using the method of Coogan and co-workers, with slight modifications, the reactions of the Schiff base of isatin and aniline (**L1**; $C_{14}H_{10}N_2O$; 41 %) with $Re(CO)_5X$ (X = Cl; **a** and Br; **b**) in toluene yielded the complexes $[Re(C_{14}H_{10}N_2O)(CO)_3X]$ (**2a**, **2b**; 96 % and 90 % respectively). Refluxing in dry toluene under nitrogen and recrystallization afforded **2b** crystallizing as a solvate compound $[Re(C_{14}H_{10}N_2O)(CO)_3Br].C_2H_5OH$ (**3**; 72 %) in ethanol. The reaction of Complex **2b** with $AgBF_4$ in diethyl ether under nitrogen yielded $[Re(C_{14}H_{10}N_2O)(C_4H_{10}O)(CO)_3]^+BF_4^-$ (**4**). Characterization was done by Fourier Transform Infra-red Spectroscopy (FTIR), Electronic spectra, Magnetic susceptibility measurements and melting point determinations. The NMR and Mass Spectra analyses were also done for **L1** and **2a**. *In-vitro* antimicrobial studies was done using three gram-positive bacteria (*Staphylococcus aureus*, *Bacillus subtilis* and haemolytic *Staphylococcus aureus*), three gram-negative bacteria (*Pseudomonas aeruginosa*, *Escherichia coli* and *Klebsiella* sp.) and three fungi (*Aspergillus niger*, *Trichoderma viride* and *Penicillium citrinum*). Complex **2a** showed a broad-spectrum activity, **2b** had activities against all gram-negative bacteria (and it was the most active against *Pseudomonas aeruginosa*) and **2c** was active against all tested gram positive bacteria. Complex **2b** had the minimum inhibitory concentration (MIC) value of 1.25 μg/mL against *Pseudomonas aeruginosa.* The tested complexes showed selective activities in a distinct manner from the ligand and mostly with higher zones of inhibition against tested organisms than tetracycline (standard clinical antibiotic) against the tested bacteria. All compounds were inactive against the tested fungi.
Keywords: 3-(phenylimino)indole-2-one, Re(I) tricarbonyl Complexes, Antimicrobial, Antifungal, Activities

1.0 INTRODUCTION

The design of metal compounds as drugs and diagnostic agents such as metal-mediated antibiotics, antibacterial, antiviral, antiparasitic, radio-sensitizing agents and anticancer compounds has recently aroused a significant rising interest [1]. Isatin is an endogenous indole with a variety of pharmacological actions, including anti-convulsant, anti-microbial and antiviral activities, inhibition of monoamine oxidase [1]. The study of the Schiff base ligands derived from isatin, their metal complexes and their biological applications has also received much attention [2,3,4,5,6,7]. Isatin-thiosemicarbazone Copper(II) complexes related to the antiviral drug, methisazone, have been prepared and characterized using spectroscopic techniques [8]. These types of complexes were found to cause significant inhibition of human leukemic cell proliferation [9], presenting the copper atom in a square pyramidal coordination, as determined by crystallographic analysis [1]. Novel biologically active Re(I) tricarbonyl complexes of 2-pyridyl-1,2,3-triazole derivatives have been reported [10]. In 2008, Amoroso *et al* prepared a novel 3-chloromethylpyridyl bipyridine tricarbonyl rhenium complex and demonstrated the biological significance of this complex in mitochondria [11]. That literature represents the first application of a luminescent rhenium agent for specific targeting of a

biological entity in imaging. Recently, Coogan and co-workers [12,13,14,15] have also directed their research focus towards such, thus preparing more novel rhenium tricarbonyl compounds to prove that heavy metal complexes are not only erroneously termed poisons, but can also be useful towards preparing drugs of great biological significance to man. Therefore, this study was aimed at successfully synthesizing and characterizing new Re(I) carbonyl complexes of isatin derived Schiff bases, predicting their coordination properties and studying their antimicrobial activities as a preliminary study for the medicinal significance of these complexes.

2.0 Experimental

2.1 Chemical

Isatin, aniline, $Re(CO)_5Cl$ and $Re_2(CO)_{10}$ were obtained from Aldrich. All solvents used (methanol, ethanol, acetone, chloroform, dichloromethane, diethyl ether, n-hexane, pyridine and *N*,*N*-dimethylformamide; DMF) were purchased as analytical grades from Sigma-Aldrich and SAARChem.

2.2 Instrumentation

The ^{1}H NMR (400 MHz) and ^{13}C NMR (500 MHz) spectra were recorded at room temperature on Bruker Spectrometers and Mercury (300 MHz) spectrometer. The Infrared spectra were recorded on a Shimadzu IRAffinity-1 spectrometer with a pike MIRacle ATR system (diamond crystal) in the range 4000 – 400 cm^{-1}. The UV-Visible spectra were recorded on a Shimadzu UV-1800 spectrometer. Mass spectra were determined using an Applied Biosystem STR Voyager (MALDI-TOFMS) instrument, equipped with a nitrogen laser (337 nm, 3 ns pulse, 20 Hz maximum firing rate). Room temperature magnetic susceptibility was determined by Johnson Matthey Magnetic Susceptibility balance. The end point of reactions and purity of the compounds was checked by Thin-Layer Chromatography (TLC) carried out on Silica Gel 60 F254 alumina plates (E Merk) using appropriate solvent mixtures of diethyl ether: petroleum ether or chloroform as the eluent and visualized in UV chamber (365 nm). Air and water sensitive compounds were weighted inside MBraun Lab Master 130 Glove box under nitrogen gas. Light sensitive reactions were carried out at night with the apparatus covered with aluminium foil paper and the hood also covered. Flash Column Chromatographic purification of compounds was done using a mixture of chloroform: diethyl ether (either 50 %: 50 % or 60 %: 40 %). The melting points of compounds were determined using a Gallenkemp variable heater apparatus or an OptiMelt MPA 100 apparatus.

2.3.0 Biological

2.3.1 Antimicrobial Activity

All synthesized compounds were screened for *in vitro* antibacterial and antifungal activities using Mueller-Hinton agar (MHA) and Potato dextrose agar (PDA) media. The antibacterial activity was evaluated against three Gram-positive bacteria (*Staphylococcus aureus*, *Bacillus subtilis* and Haemolytic *Staphylococcus aureus*) and three Gram-negative bacteria (*Pseudomonas aeruginosa*, *Escherichia coli* and *Klebsiella* sp.). The antifungal activities of the compounds were evaluated against three fungi (*Aspergillus niger*, *Trichoderma viride* and *Penicillium citrinum*). Preliminary identification of the bacteria was carried out at Bowen University, Iwo, Nigeria, following the methods described by Cheesbrough in 2002 [16]. Tetracycline (30 µg; antibiotic test kit) was used as a standard drug for the bacteria, while dimethylformamide (DMF) was used as control.

2.3.2 Antibacterial test

The preparation of each test bacteria was done according to NCCLS, 1993 [17]. The antibacterial susceptibility test was also carried out according to NCCLS procedure in 1993 [17]. The disc diffusion method [18] was used to evaluate the antimicrobial activities of the compounds using filter paper discs of diameter 8 mm and dissolved synthesized compounds in dimethylformamide (DMF) at a concentration of 100 µg/mL. Antibacterial

activity was evaluated by measuring the diameters of zones of growth inhibition in triplicates and the mean of three results was taken.

2.3.3 Antifungal test

The fungal isolates were allowed to grow on Potato dextrose agar (PDA) (LabM) at 25 °C for 5 – 7 days to sporulate. The fungal spores were harvested after sporulation by pouring a mixture of sterile glycerol and distilled water onto the surface of the plate. The spores were scraped using a sterile glass rod. The harvested fungal spores were standardized to 10^6 spores per ml. One millilitre of the standardized spore suspension was evenly spread on solidified PDA (LabM) plates using a glass spreader. The plates were placed on the work bench for 1h for the spore suspension to diffuse into the agar. The sterile discs were impregnated with the test compounds and placed aseptically using sterile forceps on the surface of the agar plates. The plates were then allowed to stand on the laboratory bench for 1 h to allow for proper diffusion of the compounds into the media. Plates were incubated at 25 °C for 96 h and observed for zones of inhibition. Activity was evaluated by measuring the diameters of zones of growth inhibition in triplicates and the mean of three results were taken.

2.4.0 Syntheses

2.4.1 Preparation of $C_{14}H_{10}N_2O$ (L1)

L1 was prepared according to the method of Subari *et al.*, 2010 [19] with slight modifications [20]. Isatin (5.0000 g; 0.3398 mol) was added to 180 mL methanol and refluxed until complete dissolution. Aniline (3.1 ml; 0.3398 mol) was added while stirring at room temperature with 8 drops of conc. H_2SO_4 added. Stirring was done for about 2 h. The light yellow solid which appeared was filtered under vacuum to give 4.32 g (0.0195 mol: 57 % yield), which on recrystallization in ethanol: chloroform (70: 30) gave 3.08 g (0.0139 mol: 41 % yield).

2.4.2 Preparation of $[Re(C_{14}H_{10}N_2O)(CO)_3Cl]$ (2a)

L1 (0.03 g; 0.14 mmol) and $Re(CO)_5Cl$ (0.05 g; 0.14 mmol) were added to 20 mL of toluene in a quick fit flask. The mixture was stirred at 100 ^{0}C for 3 h (11). The color changed from light yellow to pink within 5 min. The reaction was monitored with TLC and allowed to cool. The light purple solid produced was filtered out under vacuum and it weighed 0.07 g (0.13 mmol; 96 % yield).

2.4.3 Preparation of $[Re(C_{14}H_{10}N_2O)(CO)_3Br]$ (2b)

$Re(CO)_5Br$ (0.45 g; 1.11 mmol; prepared from $Re_2(CO)_{10}$ according to the method of Angelici, 1990) [21] was added to L1 (0.25 g; 1.11 mmol) and 45 mL toluene in a quick fit flask and refluxed for 1 h. The precipitate was then cooled outside the oil bath. The purple amorphous solid produced was filtered under vacuum yielding 0.57 g (0.99 mmol; 90 %).

2.4.4 Preparation of $[Re(C_{14}H_{10}N_2O)(CO)_3Br].C_2H_5OH$ (3)

L1 (0.0535 g; 0.2406 mmol) was added to $Re(CO)_5Br$ (0.0913 g; 0.2406 mmol) and 6 mL toluene in a quick fit flask and refluxed for 1 h under nitrogen. The mixture was cooled outside the oil bath and the pale purple precipitate was filtered under vacuum. It weighed 0.1183 g (0.1914 mmol; 79 %). Recrystallization was done in a mixture of ethanol: chloroform (70: 30).

2.4.5 Preparation of $[Re(C_{14}H_{10}N_2O)(C_4H_{10}O)(CO)_3]^+BF_4^-$ (4)

This synthesis was carried out with slight modifications to the method of Coogan and coworkers, 2009 [12]. $AgBF_4$ (0.16 g; 0.28 mmol) was added to compound **2b** (0.05 g; 0.28 mmol) and 11 mL diethyl ether in a quick fit flask under nitrogen. Stirring was done for 20 min at room temperature. Nothing happened and no color change was observed. The reaction was then refluxed. White AgBr started appearing within 10 min. The mixture was refluxed for 35 min, within which time some red precipitate also appeared. The clear solution at the top was filtered through celite and used for the next reaction. 10 mL dry THF was added to the precipitate. This was filtered through celite to remove the white AgBr precipitate. To a small portion of the filtrate was added petroleum ether to precipitate out the

compound. The red precipitate appearing at the bottom was filtered out and it weighed 0.005 g (0.008 mmol; 3 %).

3.0 Results and Discussion

Isatin was separately condensed with aniline at room temperature [20] to give **L1**. The scheme of this reaction is presented as Scheme 1.

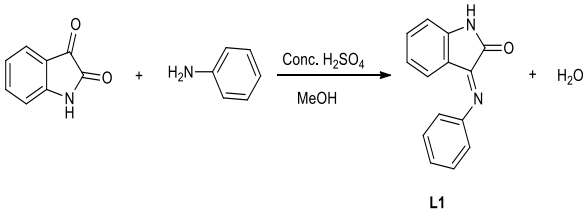

Scheme 1: Reaction for the preparation of **L1**

The equation for the preparations of complexes **2a**, **2b** and **3** is presented as Scheme 2.

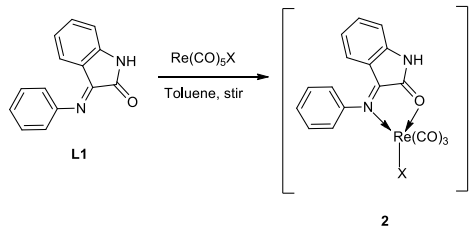

2a; X = Cl, Toluene, Stir, 100 °C, 3 h
2b; X = Br, Toluene, Reflux, 1 h
[$Re(C_{14}H_{10}N_2O)(CO)_3Br$].$C_2H_5OH$ (**3**); X = Br, Toluene, Reflux, 1 h, N_2, Recrystallized in Ethanol: Chloroform (70: 30)

Scheme 2: Scheme of reaction for the preparation of Complexes **2a**, **2b** and **3**

The reaction of complex **2b** with $AgBF_4$ in diethyl ether yielded compound **4** and it is presented as Scheme 3 below.

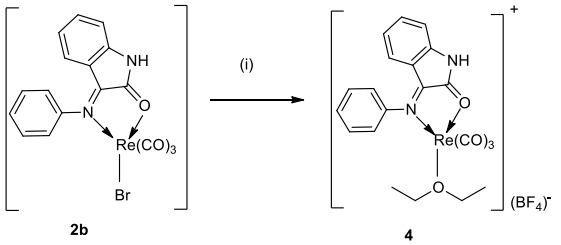

(i) $AgBF_4$, diethyl ether, Stirred 20 min, Refluxed 35 min

Scheme 3: Scheme of reaction for the preparation of complex **4**

The physical properties of the prepared rhenium carbonyl complexes and **L1** are presented in Table 1.

Table 1: Some Physicochemical properties of **L1** and its complexes

Compound	Formula (g/mol)	Colour	Melting Point (^{0}C)	% Yield
L1 ($C_{14}H_{10}N_2O$)	222	Light Yellow	213 – 215	57
[$Re(C_{14}H_{10}N_2O)(CO)_3Cl$] (**2a**)	528	Light Purple	> 320	96
[$Re(C_{14}H_{10}N_2O)(CO)_3Br$] (**2b**)	572	Purple	315 – 318	90
[$Re(C_{14}H_{10}N_2O)(CO)_3Br$].$C_2H_5OH$ (**3**)	618	Pale Purple	304– 306	79

3.1.0 Infrared spectra of Rhenium carbonyl complexes

The characteristic vibrational frequencies have been identified by comparing the spectrum of the Schiff base with the rhenium(I) carbonyl adducts. These have been presented in Table 2. The assignments of these absorption bands have also been made by comparing the spectra of the compounds with reported literature on transition metal complexes of isatin Schiff bases [4,5]. There are two potential donor sites in **L1**. These are the isatin nitrogen and the isatin oxygen. The FTIR spectrum of **L1** ($C_{14}H_{10}N_2O$) shows a medium intensity band at 3086 cm^{-1} attributed to υ(NH) stretching vibration. This band was unchanged in the spectrum of its metal carbonyl adduct, **2a**; [$Re(C_{14}H_{10}N_2O)(CO)_3Cl$], while it moved to a higher frequency of 3117 cm^{-1} in the spectra of compounds **2b**; [$Re(C_{14}H_{10}NSS_2O)(CO)_3Br$] and **3**; [$Re(C_{14}H_{10}N_2O)_2(CO)_3Br$].$C_2H_5OH$. This band at 3086 cm^{-1} moved to a higher frequency of 3287 cm^{-1} in **4**; [$Re(C_{14}H_{10}N_2O)(C_4H_{10}O)(CO)_3]^+BF_4^-$. The expected new υ(CO) stretching vibration appeared at 1906 cm^{-1} (a strong band), 1939 cm^{-1} (a shoulder band) and 2029 cm^{-1} (a strong band) in the spectrum of **2a**; [$Re(C_{14}H_{10}N_2O)(CO)_3Cl$]. In the spectrum of compound **2b**; [$Re(C_{14}H_{10}N_2O)(CO)_3Br$], these new υ(CO) stretching vibration appeared at 1898 cm^{-1} (a strong band), 1929 cm^{-1} (a shoulder band) and 2029 cm^{-1} (a strong band). The new υ(CO) stretching vibration appeared as a strong band at 1906 cm^{-1}, a shoulder band at 1924 cm^{-1} and a strong band at 2029 cm^{-1} in the spectrum of **3**; [$Re(C_{14}H_{10}N_2O_2)(CO)_3Br$].$C_2H_5OH$. The new υ(CO) bands appeared as a strong band at 1898 cm^{-1} and a medium band at 2021 cm^{-1} in the spectrum of **4.**

Table 2: Relevant Infrared Spectral Data of the L1 and its Re(I) tricarbonyl Complexes

Compound	υ(NH) (cm^{-1})	υ(CO) (cm^{-1})	υ(C=O) (cm^{-1})	υ(C=N+C=C) (cm^{-1})	υ(CH)bend (cm^{-1})	υ(C-N+C-C) (cm^{-1})	δ(M-C-O) (cm^{-1})	υ(M-N) (cm^{-1})
L1 ($C_{14}H_{10}N_2O$)	3086s	-	1736s	1605s 1651m	1458m	1096m	-	-
Compound **2a**; [$Re(C_{14}H_{10}N_2O)(CO)_3Cl$]	3086b,w	1906s 1939sh 2029s	-	1605m 1675m	1455m	1098m	576w	443m
Compound **2b**; [$Re(C_{14}H_{10}N_2O)(CO)_3Br$]	3117b, m	1898s 1929sh 2029s	-	1674s 1597m	1458s	1096m	571w	432m
Compound **3**; [$Re(C_{14}H_{10}N_2O)(CO)_3Br$].$C_2H_5OH$	3117w	1906s 1924sh 2029s	-	1674s 1597m	1458m	1096w	571w	494w
Compound **4**; [$Re(C_{14}H_{10}N_2O)(C_4H_{10}O)(CO)_3]^+BF_4^-$	3287w	1898s, 2021m	-	1682w 1614sh	1489w	1068s	579w	478s

Note: υ stretching; δ deformation; m, medium; w, weak; b, broad; sh, shoulder and s, strong

All these new υ(CO) bands are diagnostic of terminal carbonyl groups, thus ascertaining the formation of these rhenium(I) carbonyl complexes [21]. The strong υ(C=O) stretching vibration band appearing at 1736 cm^{-1} in the spectrum of L1 completely disappeared in all its rhenium carbonyl complexes. This signifies the involvement of the oxygen of the C=O in chelation. The uncoordinated C = N and C = C stretching vibrations, υ(C = N + C = C), occurred as overlapped bands at 1605 cm^{-1} and 1651 cm^{-1} [6], which eventually either underwent no change and a shift to a higher frequency of 1605 cm^{-1} and 1674 cm^{-1} in the spectrum of **2a** or underwent a shift to a lower and higher frequency of 1597 cm^{-1} and 1674 cm^{-1} in the spectra of compound **2b** and **3**; respectively on coordination to the metal ion. The υ(C=N + C=C) stretching vibration bands also underwent a shift to higher and lower frequencies of 1682 cm^{-1} and 1614 cm^{-1} in **5**; $[Re(C_{14}H_{10}N_2O)(C_4H_{10}O)(CO)_3]^+BF_4^-$ on coordination to the rhenium(I) metal ion. The medium band appearing at 1458 cm^{-1} in the spectrum of L1 was attributed to $\upsilon(CH)_{bend}$ vibrational band. This band remained unchanged in complexes **2b** and **3**. This signifies no involvement of this bond in coordination as expected.

This band also either underwent a shift to a slightly lower frequency of 1455 cm^{-1} in **2a** or a shift to a higher frequency of 1489 cm^{-1} in **4**. The new band appearing at 571 cm^{-1}, in the spectra of complexes **2b** and **3** is attributable to δ(M-C-O) bending mode [21]. This new band appeared at 579 cm^{-1} in the spectrum of **4**. The new bands appearing between 432 cm^{-1} and 494 cm^{-1} in the spectra of the complexes are attributable to υ(M-N) vibrational bands. All these ascertain the formation of these new metal carbonyls.

3.1.1 Infra-red band of the tetraflouroborate anion (BF_4^-): Cation / anion interactions can also be evidenced by a deformation of an IR band of the BF_4^- anion [22]. Usually, the highly symmetrical BF_4^- (Td) ion shows only one IR active band. For complex **4**, this is not the case. Rather, in accordance with other literature reports [22], the signal splits and a shoulder was also observed. The split $\upsilon(BF_4^-)$ band appeared at 1057 cm^{-1} and 992 cm^{-1} in $[Re(C_{14}H_{10}N_2O)(C_4H_{10}O)(CO)_3]^+BF_4^-$ (**4**).

3.2 NMR Spectra

The structure of complex **2a** is presented below as Figure 1 showing the numberings of atoms from its ligand **L1**.

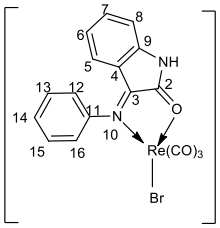

Figure 1: Structure of Complex **2b** showing the numberings of atoms from **L1**

The major stereoisomer showed the following signals (δ, ppm):7.48 (2H, m, H-13 and H-15); 7.35 (1H, td, J = 9.0 Hz and 1.2 Hz, H-6); 7.26 (1H, tt, J = 8.7 Hz and 1.2 Hz, H-14); 7.00 (3H, dt, J = 9.6 Hz and 1.2 Hz, H-5, H-12 and H-16); 6.73 (1H, td, J = 7.8 Hz and 1.2 Hz, H-7) and 6.50 (1H, dt, J = 7.8 Hz, and 0.6 Hz, H-8). The minor isomer showed the following signals (δ, ppm): 7.62 (1H, d, J = 8.1 Hz, H-5); 7.11 (4H, m, H-13 and 15; H-6 and H-7); 7.05 (3H, m, H-12 and H-16; H-14) and 6.95 (1H, d, J = 5.1 Hz, H-8). **L1** crystals were grown in ethanol and chloroform solvent mixture, hence the ethanol solvent peaks in $(CD_3)_2CO$ also appeared as follows (δ, ppm): 1.12 (3H, t, CH_3), 3.58 (2H, q, CH_2) and 3.31 (1H, s, OH). The comparison of the ^{1}H-NMR of **L1** with that of complex **2b**; $[Re(C_{14}H_{10}N_2O)(CO)_3Br]$ suggest ligand deprotonation during metal chelation. The ^{1}H-NMR spectrum of $[Re(C_{14}H_{10}N_2O)(CO)_3Br]$ showed the following signals (δ, ppm): 7.61 (6H, m, H-13 and H-15, H-12 and H-16, H-14 and H-6); 7.29 (1H, d, J = 8.1 Hz, H-5); 7.09 (1H, td, J = 7.8 and 1.2 Hz, H-7) and 6.88 (1H, dt, J = 8.7 Hz and 0.6 Hz, H-8). All these show an evidence of complexation. The other expected aromatic proton signals from the ligand appeared as follows (δ, ppm): 7.73 - 7.58 (6H, m, H-13, H-15, H-12, H-16, H-14 and H-6); 7.29 (1H, d, J = 8.1 Hz, H-8); 7.09 (1H, dd, J = 8.7 and 0.6 Hz, H-5) and 6.88 (1H, dt, J = 8.7 Hz and 0.6 Hz, H-7). In the ^{13}C-NMR spectrum of **L1**, 20 signals were observed as follows (δ, ppm): 164.1 (C = O), 155.5 (C =N), 152.0 (Cq), 150.2 (Cq), 147.7 (Cq), 134.9 (CH), 134.7 (CH), 130.3 (CH), 129.0 (CH), 126.6 (CH), 125.6 (CH), 125.3 (CH), 123.5 (CH), 123.2 (CH), 122.5 (H), 119.9 (CH), 118.0 (CH), 117.0 (CH), 112.1 (CH) and 111.4 (CH). This means that the carbon atoms of both the E and Z stereoisomers have produced the 20 signals with eight carbon atoms overlapping. In the ^{13}C-NMR spectrum of complex **2a**, 14 signals were observed. The new diagnostic signals due to the carbonyls appeared as follows (δ, ppm): 198.0 (C ≡ O), 196.1 (C ≡ O) and 187.3 (C ≡ O) [12]. Other carbon signals from **L1**, were observed as follows (δ, ppm): 163.6 (C = O; C-2), 149.6 (C = N; C-3), 148.6 (Cq; C-11), 137.9 (Cq; C-9), 130.8 (CH; C-13 & C-15), 130.1 (CH; C-5), 127.5 (CH; C-14 & C-7), 125.7 (CH; C-6), 121.3 (CH; C-8), 116.6 (CH; C-12 & C-16) and 115.2 (Cq; C4). 11 carbon signals were observed instead of 14 signals from **L1**. This signifies the overlap of 3 carbon atoms. It is expected that C-12 and C-16 will overlap, as well as C-13 and C-15. C-14 has also possibly overlapped with C-7 [4,5].These anomalous behaviour in the NMR spectra of **L1** and its complex **2a** were further established by the single crystal x-ray analysis, whose data was the same as previously reported by Al Subari (2010). Therefore the x-ray analysis also confirmed that the target compound, L1 was formed, purified and used for this research.

3.3 Mass Spectra

In the mass spectrum of L1 significant peaks were observed at $^m/_z$ (ESI) 451 (100 %), $^m/_z$ 247 (41 %), $^m/_z$ 229 (5 %), $^m/_z$ 223 (24 %, molecular ion), $^m/_z$ 143 (14 %) and $^m/_z$ 127 (91 %). The base peak appearing at $^m/_z$ 451 is due to 2 moles of the ligand with 1mole of Lithium (Li; used for the analysis). Thus $^m/_z$ 451 corresponds to $[2M+Li+H]^+$. This ion at $^m/_z$ 451 loses $C_{14}H_8N_2$ (204 mass units) to yield the ion at $^m/_z$ 247 (41 %) corresponding to $[2M+Li-C_{14}H_8N_2+H]^+$, which is the same as $[M+H_2O+Li+H]^+$. This is followed by loss of H_2O (18 mass units) to give an ion at $^m/_z$ 229 (50 %) corresponding to $[M+Li+H]^+$, which fragments further by loss of Li (7 mass units) and then addition of proton (H) to

give an ion at $^{m}/_{z}$ 223 (24 %) corresponding to $[MH]^+$. The ion at $^{m}/_{z}$ 223 fragments by loss of C_6H_6 (78 mass units) and then H_2 (2 mass units) with an addition of a proton to give the ion at $^{m}/_{z}$ 143 (14 %), which corresponds to $[M-C_6H_6-H_2+H]^+$. The ion at $^{m}/_{z}$ 143 fragments further by the loss of CH_4 (16 mass units) followed by the addition of proton (H; 1 mass unit) to yield the ion at $^{m}/_{z}$ 127 (91 %) corresponding to $[M-C_6H_6-H_2-CH_4+H]^+$. The mass spectral data are collected in Table 3, while the fragmentation pattern is shown in Scheme 3.

Table 3: Mass Spectral Fragmentation of L1 ($C_{14}H_{10}N_2O$)

$^{M}/_{Z}$	Fragment
451	$[2M+Li+H]^+$
247	$[2M+Li-C_{14}H_8N_2+H]^+$ OR $[M+H_2O+Li+H]^+$
229	$[M+Li+H]^+$
223	$[M+H]^+$
143	$[M-C_6H_6-H_2+H]^+$
127	$[M-C_6H_6-H_2-CH_4+H]^+$

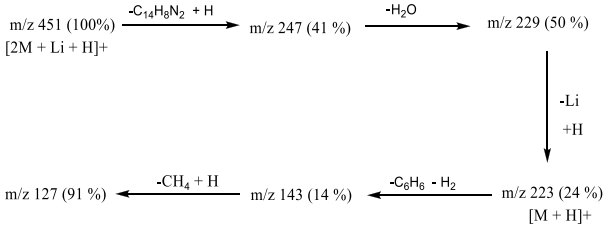

Scheme 3: Fragmentation route for **L1**

In the mass spectrum of Complex **2b**; $[Re(C_{14}H_{10}N_2O)(CO)_3Br]$, the expected molecular ion appeared at $^{m}/_{z}$ 572 (45 %). This ascertains a 1:1 complexation as expected. The highest peak in the mass spectrum of this complex appearing at $^{m}/_{z}$ 781 (20 %) is due to side reactions involving the addition of 2,4,6 – trihydroxyacetophenone (THAP) during the analysis. The molecular ion fragments via two routes as follows:

(i) The loss of 2CO (56 mass units) with the addition of a proton (H; 1 mass unit) from the molecular ion gives the ion with the peak at $^{m}/_{z}$ 517 (25 %) corresponding to $[M-2CO+H]^+$. The loss of Bromine radical ($Br^{\cdot}$; 80 mass units) and further loss of proton (H; 1 mass unit) from this ion yields another ion at peak $^{m}/_{z}$ 436 (10 %) corresponding to $[M-2CO-Br^{\cdot}]^+$. The ion at $^{m}/_{z}$ 436 loses C_6H_6 (72 mass units) to yield another ion at peak $^{m}/_{z}$ 358 (12 %) corresponding to $[M-2CO-Br^{\cdot}-C_6H_6]^+$. Alternatively, when the ion at $^{m}/_{z}$ 436 loses CO (28 mass units) with a concomitant loss of C_3H_8 (44 mass units) and the addition of proton (H; 1 mass unit) it yields another ion at peak $^{m}/_{z}$ 365 (5 %) corresponding to $[M-3CO-Br^{\cdot}-C_3H_8+H]^+$. The ion at $^{m}/_{z}$ 365 also fragments by loss of C_2H_6 (30 mass units) followed by loss of proton (H; 1 mass unit) to give the base peak ion at $^{m}/_{z}$ 334 (100 %) corresponding to $[M-3CO-Br^{\cdot}-C_3H_8-C_2H_6]^+$.

(ii) The molecular ion loses 3CO (84 mass units) followed by a concomitant loss of bromine radical ($Br^{\cdot}$; 80 mass units) and a loss of C_4H_{10} (58 mass units) to yield the ion at peak $^{m}/_{z}$ 350 (72 %) corresponding to $[M-3CO-Br^{\cdot}-C_4H_{10}]^+$. The ion at peak $^{m}/_{z}$ 350 loses CH_4 to yield the base peak ion $^{m}/_{z}$ 334 (100 %) corresponding to $[M-3CO-Br^{\cdot}-C_4H_{10}-CH_4]^+$. The spectral fragmentation is presented in Table 4, while the fragmentation pattern is presented in Scheme 4.

Table 4: Mass Spectral Fragmentation of Compound 2b; $[Re(C_{14}H_{10}N_2O)(CO)_3Br]$

$^{M}/_{Z}$	Fragment
572	$[M]^+$
517	$[M-2CO+H]^+$
436	$[M-2CO-Br]^+$
365	$[M-3CO-Br-C_3H_8+H]^+$
358	$[M-2CO-Br-C_6H_6]^+$
350	$[M-3CO-Br-C_4H_{10}]^+$
334	$[M-3CO-Br-C_4H_{10}-CH_4]^+$ or $[M-3CO-Br-C_3H_8-C_2H_6]^+$

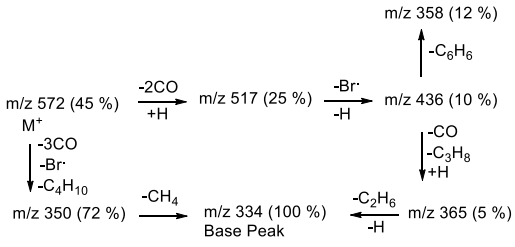

Scheme 4: Fragmentation pattern of Complex **2b**: $[Re(C_{14}H_{10}N_2O)(CO)_3Br]$

3.4 Magnetic susceptibility Measurement

The magnetic moments for the prepared complexes were measured at room temperature. The value was 0 B.M for the rhenium carbonyl adducts showing that these complexes are diamagnetic. This value signifies the following:
(a) since Re(I) is in the d^6 electronic state, the complexes will assume an octahedral shape;
(b) L1 is a strong field ligand and
(c) the prepared rhenium carbonyl complexes are low spin.

3.5 Electronic spectra

The electronic spectra data for **L1**, **2a**, **2b** and **3** as determined in methanol is presented as Table 5. The maximum absorption bands (λ_{max}) for these compounds have also been determined in methanol.

Table 5: Electronic Spectra of L1 and its Re(I) tricarbonyl Complexes

Compound	Band Position (nm)	Molar Absorptivity ($M^{-1}cm^{-1}$) (E; M^{-1} cm^{-1})	Band Position (cm^{-1})	Band Assignment
L1 ($C_{14}H_{10}N_2O$)	406 296 246	2,588 4,892 24,024	26,631 33,784 40,650	n –π* π –π* π –π*
Complex **2a** [Re($C_{14}H_{10}N_2O$)$(CO)_3$Cl]	459 316 254	7,211 6,404 12,422	21,786 31,646 39,370	MLCT π –π* π –π*
Complex **2b** [Re($C_{14}H_{10}N_2O$)$(CO)_3$Br]	472 328 249	5,664 6,261 20,073	21,231 30,489 40,161	MLCT π –π* π –π*
Complex **3** [Re($C_{14}H_{10}N_2O$)$(CO)_3$Br]. C_2H_5OH	471 328 251	11,965 13,480 24,691	21,231 30,489 39,840	MLCT π –π* π –π*

The λ_{max} for **L1** is 409 nm (26,631 cm^{-1}) with a molar absorptivity value (E) of 2,588$M^{-1}cm^{-1}$. This is expected due to the extended conjugation which could also include the C=N after deprotonating nitrogen in the indole ring of isatin, thus also presenting the tautomeric enol form of **L1** in solution [5]. The λ_{max} for **2a** is 459 nm (21,786 cm^{-1}) with the molar absorptivity value of 7,211 $M^{-1}cm^{-1}$. The λ_{max} for **2b** is 472 nm (21,231 cm^{-1}) with the molar absorptivity value of 5,664 $M^{-1}cm^{-1}$. The λ_{max} for **3** is 471 nm (21,231 cm^{-1}) with the molar absorptivity value of 11,965 $M^{-1}cm^{-1}$. The ultraviolet spectrum of **L1** showed absorption bands at 33,784 $cm^{-1}$and 40,650 cm^{-1} which have been assigned to π – π* transition [23]. The band appearing at 24,631 cm^{-1} is attributable to n – π* transition. The interpretations of ultraviolet spectra of metal complexes of isatin derived Schiff bases revealed that charge – transfer bands occur in the same region with π – π* transitions [4]. The ultraviolet spectra of the rhenium carbonyl complex **2a**; [Re($C_{14}H_{10}N_2O$)$(CO)_3$Br] was therefore characterized by absorption bands at 31,646 cm^{-1} and 39,370 cm^{-1} assigned to ligand π – π* transitions [23]. The absorption band appearing at 21,786 cm^{-1} has been assigned to MLCT {dπ(Re) – π*} transition. Complex **2b**; [Re($C_{14}H_{10}N_2O$)$(CO)_3$Br] was also characterized by absorption bands at 30,489 cm^{-1} and 40,161 cm^{-1} assigned to ligand π – π* transitions [22]. The absorption band appearing at 21,231 cm^{-1} has been assigned to MLCT {dπ(Re) – π*} transition. Complex **3**; [Re($C_{14}H_{10}N_2O$)$(CO)_3$Br].C_2H_5OH was characterized by absorption bands at 30,489 cm^{-1} and 39,840 cm^{-1} assigned to ligand π – π* transitions. The absorption band appearing at 21,231 cm^{-1} has been assigned to MLCT {dπ(Re) – π*} transition. All these are consistent with the magnetic moment of 0 as determined for these complexes and a low spin octahedral configuration.

3.6 Elemental Analysis

The result of the elemental analysis carried out for complex **3** is presented below. This result revealed that this compound is only a solvate compound of **2b**, similar to an earlier report in literature [24].

Compound 3;
[Re($C_{14}H_{10}N_2O$)$(CO)_3$Br].C_2H_5OH
Found (Calculated Values; %): C: 36.39 (36.90); H: 3.61 (2.61); N: 5.02 (4.53); O: 12.26 (12.36).

3.7.0 Antibacterial Studies

The results from the antibacterial activities of **L1** and its rhenium carbonyl complexes are presented in Table 4 and also displayed

in Figure 2. Compound **2a** showed a broad spectrum with higher zones of inhibition than tetracycline against tested bacteria except *Klebsiella sp*. Thus this rhenium complex can be a target broad spectrum antibiotic. Compound **2b** was active against the three gram negative bacteria and the most effective of the rhenium complexes against the drug resistant *Pseudomonas aeruginosa* [25, 26]. Thus it could be developed as a drug against gram negative bacteria particularly anti-*Pseudomonas* drug. Compound **2b** was also active against *Staphylococcus aureus* with a higher activity than tetracycline. Compound **3** was active against all tested gram positive bacteria (*Bacillus subtillis*, *Staphylococcus aureus* and Heamolytic *Staphylococcus aureus)* with much higher zones of inhibition than tetracycline. Thus it could be a target gram positive antibiotic.

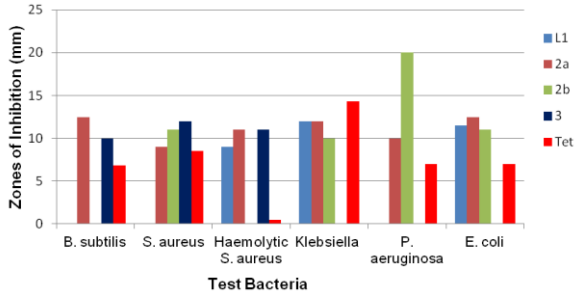

Note Keys:

L1 = $C_{14}H_{10}N_2O$ **2a** = $[Re(C_{14}H_{10}N_2O)(CO)_3Cl]$

2b = $[Re(C_{14}H_{10}N_2O)(CO)_3Br]$

3 = $[Re(C_{14}H_{10}N_2O)(CO)_3Br].C_2H_5OH$

Figure 2: Antibacterial Activities of **L1** and its Rhenium Carbonyl Complexes

3.7.1 Minimum Inhibitory Concentration (MIC)

The MIC was carried out for **2b**, which had the highest zone of inhibition against the drug resistant gram negative bacterium *Pseudomonas aeruginosa* (25, 26). This was determined by adding 10, 5.0, 2.5, 1.25, 0.625, and 0.3125 µg/ml of the complex into test tubes containing sterile nutrient broth. The microorganism was then introduced into the broths containing different concentrations of the complex. The tubes were then incubated for 24 h at 37 ^oC. The MIC was taken as the lowest concentration of the extracts that did not permit any visible growth [27]. Complex **2b** had the MIC value of 1.25 µg/ml against *Pseudomonas aeruginosa*.

3.7.2 Antifungal Studies

The results of the antifungal studies revealed that all the tested compounds were inactive against the tested fungi.

4.0 Conclusion

The isatin Schiff base of aniline (**L1**) has been successfully coordinated to form some Re(I) tricarbonyl complexes. **L1** has behaved as a bidentate ligand with Re(I), coordinating through the azomethine nitrogen and keto oxygen in all the complexes **2a**, **2b**, **3** and **4**. These complexes were found to be diamagnetic. The complexes were therefore assigned as low spin, 6-coordinate complexes assuming octahedral geometry. The proposed structures of these complexes are therefore presented in Figure 3 below corroborated with spectra and physicochemical data including melting points (Table 1). These spectra data are IR data (Table 2), Mass spectra data (Tables 3), Electronic spectra data (Table 4), Magnetic moment and Elemental analyses. Antibacterial studies revealed that **2a** had a broad spectrum with a much better activity against tested bacteria than tetracycline (standard clinical antibiotic). **L1** was active against *Klebsiella* sp. and *Escherichia coli*. Compound **2b** was active against all the tested gram negative bacteria and most effective against *Pseudomonas aeruginosa*. **2b** could therefore be a target antibiotic against gram negative bacteria, most especially *Pseudomonas aeruginosa*. Complex **3** was active against all tested gram positive bacteria with much higher zones of inhibition than tetracycline. The antimicrobial studies of these complexes revealed immerse improved activities than that of their ligand (**L1**). These complexes therefore showed significant biological implications in medicine. Complexes **2a**, **2b** and their Schiff base, **L1** showed significant inhibitory activities against the growth of tested gram negative bacteria, therefore they

can be recommended for further applications in cell imaging.

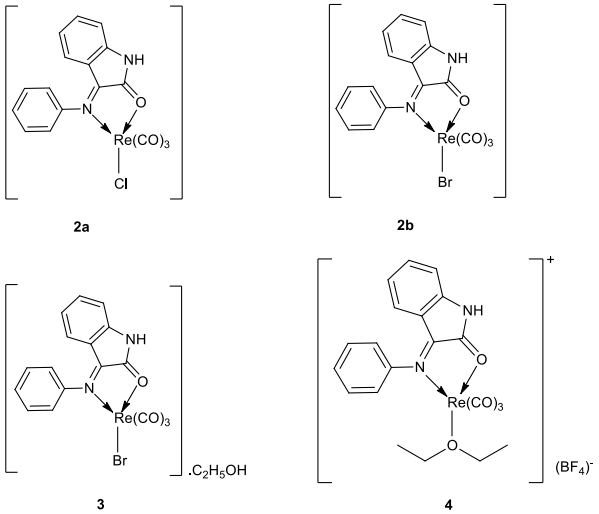

Figure 3: Proposed structures of rhenium(I) tricarbonyl complexes of **L1**

Acknowledgements

We thank Prof. John A. Gladysz for providing facilities for a portion of these studies, and helpful discussions.

Funding

The US National Science Foundation (NSF, CHE 1153085) is thanked for supporting the portion of the research carried out at Texas A & M University.

Conflict of Interests

The authors have no conflict of interests to declare.

References

[1] C. Giselle, C. F. Ana Maria (2006). Oxindoles and copper complexes with oxindole-derivatives as potential pharmacological agents, J. Braz. Chem. Soc. 17, 1473-1485.

[2] B. T. Khan, K. Najmuddin, S. Shamsuddin, S. M. Zakeeruddin (1990). Mixed ligand complexes of cis-dichloroethionine palladium (II) with purines, pyrimidines and nucleosides, Inorg. Chim. Acta, 170, 129-131.

[3] R. V. Singh, N. Fahmi, M. K. Biyala (2005). Coordination behavior and biopotency of N and S/O donor ligands with their Paladium(II) and Platinum(II) complexes. J. Iranian Chem. Soc. 2, 40-46.

[4] Z. H. Chohan, A. U. Shaikh, M. M. Naseer (2006). Metal-based isatin-bearing Sulfonamides: their synthesis, characterization and biological properties. Appl. Organometal.Chem., 20, 729-739.

[5] A. A. Ikotun, G. O. Egharevba, C. A. Obafemi, O. O. Owoseni (2012). Ring deactivating effect on antimicrobial activities of metal complexes of the Schiff base of *p*-nitroaniline and isatin, J. Chem. Pharm. Research. 4, 416–422.

[6] A. A. Ikotun, M. P. Coogan, A. A. Owoseni, N. Bhuvanesh, G. O. Egharevba (2015). Design, Syntheses, Physicochemical and Biological Properties of Rhenium(I) tricarbonyl complexes of isatin derivative. Proceedings of the British Pharmacological Society, http://www.pA2online.org/abstracts/Vol12Issue3abst275P.pdf.

[7] Panda; Patro, V. J.; Sahoo, B. M. and Mishra, J. (2013). Green Chemistry Approach for Efficient Synthesis of Schiff Bases of Isatin Derivatives and evaluation of their Antibacterial Activites, Journal of Nanoparticles ID 549502.

[8] V. K. Sharma, A. Srivastava, S. Srivastava (2006). Synthesis, structure and tetradentate Schiff bases, J. Serb. Chem. Soc. 71, 917-928.

[9] J. S. Casas, E. E. Castellano, M. S. Garcia, A. Tasende, Sachez, J. Sordo (2000). Reaction of dimethylthallium(III) acetate and isatin-3-thiosemicarbazone crystal and molecular structure of dimethyl (dimethylsulfoxide) (isatin-3-thiosemicarbazonato) thallium(III). Inorg. Chim.Acta, 304, 283-287.

[10] Y. Aimene, R. Eychenne, S. Mallet-Ladeira, N. Saffon, J. Winum, A. Nocentini, C. T. Supuran, E. Benoist, A. Seridi (2019). Novel Re(I) tricarbonyl coordination compounds based on 2-pyridyl-1,2,3-triazole derivatives bearing a 4-amino-substituted benzenesulfonamide arm; synthesis, crystal structure, computational studies and inhibitory activity against carbonic anhydrase I, II and IX isoforms. J. Enzyme Inhib Med Chem, 34, 773-782.

[11] A. J. Amoroso, R. J. Arthur, M. P. Coogan, J. B. Court, V. Fernandez-Moreira, A. J. Hayes, D. Lloyd, C. Millet, S. J. A. Pope (2008). 3-Chloromethylpyridyl

bipyridine*fac*-tricarbonyl rhenium: a thiol-reactive luminophore for microscopy accumulates in mitochondria. New J. Chem., 32, 1097-1102.
[12] M. P. Coogan, V. Fernandez-Moreira, B. M. Kariuki, S. J. A. Pope, F. L. Thorp-Greenwood (2009). A rhenium *fac*-tricarbonyl 4'-oxo-terpy trimer as a luminescent molecular vessel with a removable silver stopper, Angew. Chem. Int. Ed. Engl. 48, 4965-4968.
[13] V. Fernandez-Moreira, F. L. Thorp-Greenwood, M. P. Coogan (2010). Application of d^6 transition metal complexes in fluorescence cell imaging, Chem. Commun. 46, 186-202.
[14] R. G. Balasingham, M. P. Coogan, F. L. Thorp-Greenwood (2011). Complexes in context: attempting to control the cellular uptake and localization of rhenium fac-tricarbonylpolypyridyl complexes, Dalton Trans. 40, 11663-11674.
[15] R. G. Balasingham, F. L. Thorp-Greenwood, C. F. Williams, M. P. Coogan, S. J. Pope (2012). Biologically compatible, phosphorescent dimetallic rhenium complexes linked through functionalized alkyl chains: syntheses, spectroscopic properties, and applications in imaging microscopy, Inorg. Chem. 51, 1419-26.
[16] Cheesbrough M. (2002). Biochemical tests to identify bacteria. In: Laboratory practice in tropical countries. CheesbroughM (ed.). Cambridge Edition, 63-87.
[17] NCCLS (National Committee for Clinical Laboratory Standards). Methods for dilution in antimicrobial susceptibility tests: Approved Standard M2-A5. Villanova, P. A., NCCLS, 1993.
[18] K.C. Emeruwa, Antimicrobial substances from *Cacaya papaya* fruit extracts (1982). J. Nat. Prod. 45, 123-127.
[19] A. Al Subari, R. Bouhfid, H. Zouihri, E. Essasi, S. Weng Ng (2010). 3-(Phenlimino)indolin-2-one. Acta Cryst. E66, 0453.
[20] A. A. Adetoye, G. O. Egharevba, C. A. Obafemi, D. R. Kelly (2009). Synthesis and physicochemical properties of Co(II), Cu(II), Fe(III), Mn(II) and Ni(II) complexes of isatin derivative of sulfanilamide. Toxicol. Environ. Chem. 91, 837-846.
[21] R. C. Angelici (2007). Inorganic Syntheses: Reagents for Transition Metal Complexes and Organometallic Syntheses. John Wiley & Sons, Inc., 1990, 28, Online version.
[22] A. Scherer (2009). Ph.D Thesis, Friedrich-Alexander Universität, Erlangen-Nürnberg, Germany.
[23] D. Sutton, Electronic Spectra of Transition Metal Complexes, McGRAW-HILL, London, 1968.
[24] G. O. Egharevba, M. Megnamisi-Belombe, H. Endres, E Rossato (1982). *Acta Cryst*., Hexaaquacobalt(II) Bis[dibromobis(ethanedialdioxamato)cobaltate(III)] Acetone solvate. Acta Cryst. B38, 2901-2903. (0567-7408/82/112901-03).
[25] R. E. W. Hancock, D. P. Speert (2000). Antibiotic resistance in *Pseudomonas aeruginosa*: mechanisms and impact on treatment. Drug Resistance Updates, 3, 247-255.
[26] J. K. Lutz, J. Lee (2011). Prevalence and Antimicrobial-Resistance of *Pseudomonas aeruginosa* in Swimming Pools and Hot Tubs. Int. J. Environ. Res. Public Health, 8, 554-564.
[27] NCCLS (National Committee for Clinical Laboratory Standards). Methods for dilution of antimicrobial susceptibility tests of bacteria that grow aerobically: Approved Standard M100-S12. Wayne, P. A., NCCLS, 2002.